Crystallographic and magnetic properties of $DyFe_{12-x}Mo_x$ $(1.00 \leqslant x \leqslant 2.75)$

1998 J. Phys.: Condens. Matter 10 4177

(http://iopscience.iop.org/0953-8984/10/19/005)

J. Phys.: Condens. Matter **10** (1998) 4177–4184. Printed in the UK PII: S0953-8984(98)88755-9

Crystallographic and magnetic properties of $DyFe_{12-x}Mo_x$ ($1.00 \leqslant x \leqslant 2.75$)

Chang-Ping Yang†, Yi-Zhong Wang†‡, Bo-Ping Hu‡ and Zhen-Xi Wang‡

† State Key Laboratory for Magnetism, Institute of Physics, Chinese Academy of Sciences, PO Box 603, Beijing 100080, People's Republic of China

‡ Sanhuan Research Laboratory, Chinese Academy of Sciences, PO Box 603, Beijing 100080, People's Republic of China

Received 22 October 1997, in final form 20 January 1998

Abstract. The $DyFe_{12-x}Mo_x$ ($1.00 \leqslant x \leqslant 2.75$) series has been investigated by means of x-ray diffraction, thermomagnetic analysis, vibrating sample magnetometer, SQUID magnetometer and the singular-point detection technique. With increasing Mo concentration, lattice parameters a, c and V increase linearly, while Curie temperature T_C and saturation magnetization M_s decreases markedly. A value of M_s of 15.2 μ_B fu^{-1} has been obtained for the hypothetical $DyFe_{12}$ compound. All the samples show uniaxial anisotropy at room temperature. A maximum appears at $x = 1.5$ on the curve of magnetocrystalline anisotropy field B_a versus Mo concentration at room temperature. At low temperature, $DyFe_{12-x}Mo_x$ compounds have a complex magnetic behaviour. A transition from uniaxial anisotropy to canted structure at low temperatures in samples with low Mo concentration ($x < 2$) and magnetohistory effects in samples with high Mo concentration ($x \geqslant 2$) were observed.

1. Introduction

The RFe_{12} (R = rare earth) compound with tetragonal structure does not exist, but the ternary intermetallics $R(Fe, M)_{12}$ could be formed if a small amount of the third element M (M = Ti, V, Cr, W, Si, Mo and Nb) is substituted for Fe [1–3]. The properties and concentration of stabilizing element M have considerable influence on the magnetic properties of $R(Fe, M)_{12}$ [2, 4]. The influence results from the contribution of extra states from the third element M into the 3d band of the Fe sublattice [5]. The $R(Fe, Mo)_{12}$ compound shows quite a difference in magnetic properties from other $R(Fe, M)_{12}$ series such as M = Ti, V, Cr, W and Si. For example, the Curie temperature decreases much more rapidly with Mo concentration than with other stabilizing elements. Besides, the magnetohistory effect was observed only in the $R(Fe, Mo)_{12}$ system [6, 7]. At present, a number of studies on magnetic properties, especially the magnetic anisotropy and magnetic phase transition, have been reported [8–13]. These investigations mainly focus on $R(Fe, Mo)_{12}$ compounds for Mo = 2 [11–13]. But a study on magnetic properties varying with Mo concentration in the heavy rare-earth $RFe_{12-x}Mo_x$ system is lacking. In the present work, we studied the effect of Mo substitution on the crystallographic and magnetic properties for the $DyFe_{12-x}Mo_x$ series in a range of temperature from 4.2 K to room temperature.

0953-8984/98/194177+08$19.50

2. Experimental details

The ingots were prepared by arc-melting the constituent elements with starting purity of 99.9%. They were melted several times to ensure homogeneity under an atmosphere of highly purified argon. 5% excess of Dy was used for compensating the loss during melting. The alloys, sealed in vacuum excavated quartz tubes, were annealed for 15 hours at 1050 °C. The quality of samples was checked by x-ray diffraction and thermomagnetic analysis (TMA). Lattice parameters and unit-cell volume were determined by indexing the x-ray diffraction patterns. Curie temperatures were measured by vibrating sample magnetometer (VSM) at a low field of 0.04 tesla. Magnetocrystalline field B_a was measured with the singular-point detector (SPD) technique [14]. The magnetization curves at 4.2 K and room temperature were obtained by SQUID and VSM in a field up to 6.5 tesla and 2.0 tesla respectively. Saturation magnetization M_s was obtained by plotting M against $1/H$ in the high-field part of the magnetization curves and extrapolating H to ∞ [15]. The magnetohistory effect was observed using VSM.

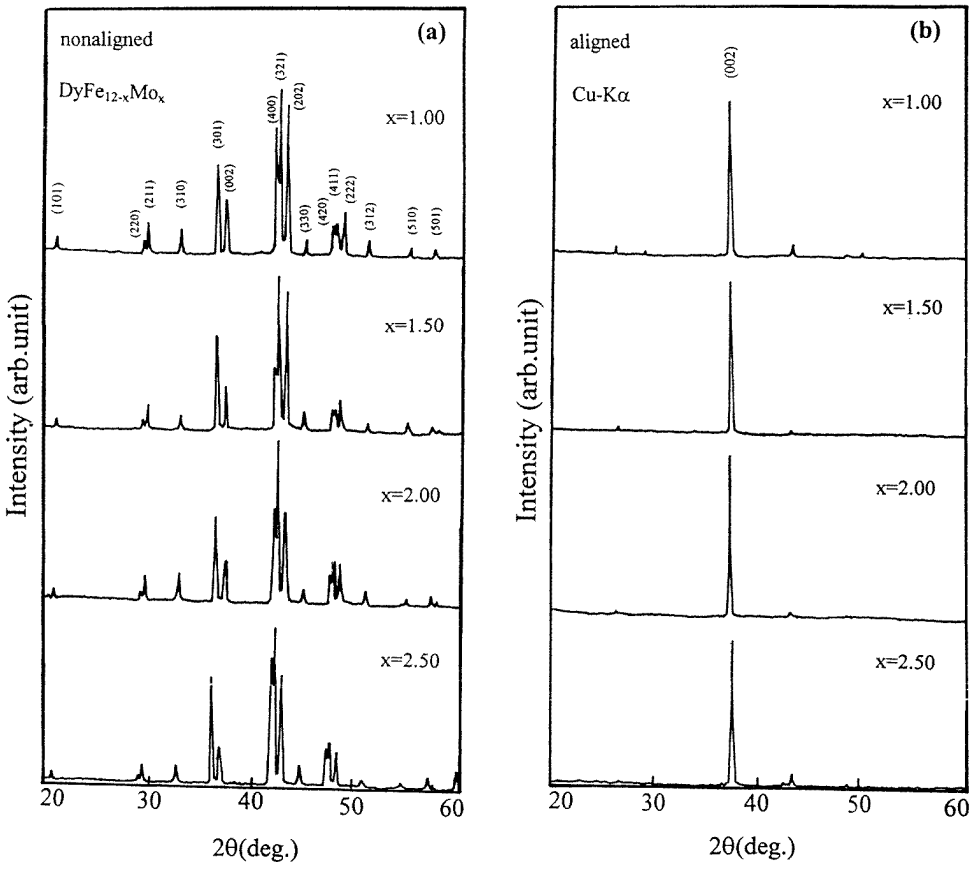

Figure 1. X-ray diffraction patterns of unaligned and aligned samples for $DyFe_{12-x}Mo_x$ series.

3. Results and discussion

The unaligned powder x-ray diffraction patterns of the $DyFe_{12-x}Mo_x$ series are shown in figure 1(a). All peaks could be indexed with a tetragonal $ThMn_{12}$ structure (space group $I4/mmm$). This indicates that all the samples are single phase with the tetragonal $ThMn_{12}$ type. The TMA data also confirmed such a conclusion. The lattice parameters a, c and unit-cell volume V are summarized in table 1 and plotted in figure 2. Fitting the data of figure 2 with least-squares methods, we can see that with increasing Mo concentration the parameters a and c increase linearly but with a different slope. The slope $\Delta a/\Delta x$ of parameter a is 0.0038 nm/Mo in comparison with 0.0026 nm/Mo for $\Delta c/\Delta x$ of parameter c. The slope of $\Delta a/\Delta x$ is larger than that of $\Delta c/\Delta x$ (about 1.5 times). It implies that the Mo substitution atoms have strong preference for the 8i sites which are located in the crystal prism along the a-axis, and result in a different expansion of a and c. This result is in good agreement with that from x-ray diffraction of $NdFe_{10}Mo_2$ [2] and neutron diffraction for $NdFe_{10}Mo_2$ [16] and $YFe_{12-x}Mo_x$ ($x = 1$–3) [17] which indicates Mo atoms prefer to occupy 8i sites in the Mo-containing systems. A similar result can be found for $YFe_{12-x}Mo_x$ in the literature [15, 18] where $\Delta a/\Delta x$ is about 1.60 and 1.72 times $\Delta c/\Delta x$ respectively.

Table 1. Crystallographic and magnetic data of $DyFe_{12-x}Mo_x$ series. Parameters a and c are the lattice constants, V is unit-cell volume, T_C is Curie temperature, M_s is saturation magnetization, n_{Dy-Fe} is molecular-field coefficient, $\mu_0 H_a$ is magnetic anisotropy field and EMD is easy magnetization direction.

					M_s (μ_B fu^{-1})			$\mu_0 H_a$ (T)	EMD	
x	a (nm)	c (nm)	V (nm)^3	T_C (K)	4.2 K	300 K	n_{Dy-Fe} (μ_0)	300 K	4.2 K	300 K
1.00	0.8513	0.4776	0.3461	490	10.76	12.37	88	0.88	canted	c-axis
1.25	0.8526	0.4787	0.3480	474	9.03	11.17	93	0.92	canted	c-axis
1.50	0.8537	0.4786	0.3488	449	8.10	9.30	87	1.03	canted	c-axis
1.75	0.8544	0.4793	0.3499	423	6.74	8.64	90	0.96	canted	c-axis
2.00	0.8559	0.4799	0.3516	373	5.74	7.59	98	0.62	canted	c-axis
2.25	0.8558	0.4801	0.3514	350	4.30	5.98	—	0.50	random	c-axis
2.50	0.8570	0.4817	0.3537	311	3.76	4.59	85	>0	random	c-axis
2.75	0.8583	0.4825	0.3547	236	1.87	2.65	—	>0	random	c-axis

The Mo concentration dependence of Curie temperature is shown in figure 3. It can be seen that Curie temperature falls markedly with increasing Mo concentration as seen in $YFe_{12-x}Mo_x$ [15, 19], more rapidly than supposed from a simple dilution of Fe by Mo. The exchange field coefficient n_{Dy-Fe} which corresponds to the contribution from Dy–Fe exchange interaction can be deduced from the molecular-field approximation [20]. Generally, neglecting the exchange interaction between rare earth, the expression of the molecular coefficient n_{Dy-Fe} is given by

$$n_{Dy-Fe} = \frac{g_J^2\sqrt{(T_C - T_{Fe})T_C}}{4(g_J - 1)^2 C_{Dy} C_{Fe}}$$

where C_{Dy} and C_{Fe} are the Curie constants for Dy and Fe sublattices respectively. Using the Curie temperature data of $DyFe_{12-x}Mo_x$ listed in table 1 and the values of T_C of $YFe_{12-x}Mo_x$ from the literature [19], the exchange field coefficient n_{Dy-Fe} can be calculated. The calculated values of n_{Dy-Fe} were listed in table 1 and plotted in figure 3 in comparison with n_{Fe-Fe} which were obtained from $YFe_{12-x}Mo_x$ [15]. It can be seen that n_{Dy-Fe} almost

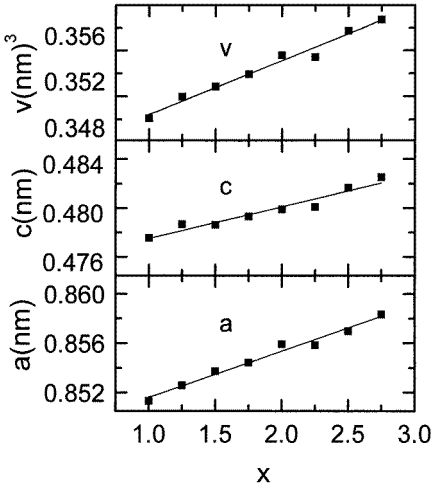

Figure 2. Mo concentration variation of lattice parameters (a and c) and unit-cell volume V for $DyFe_{12-x}Mo_x$.

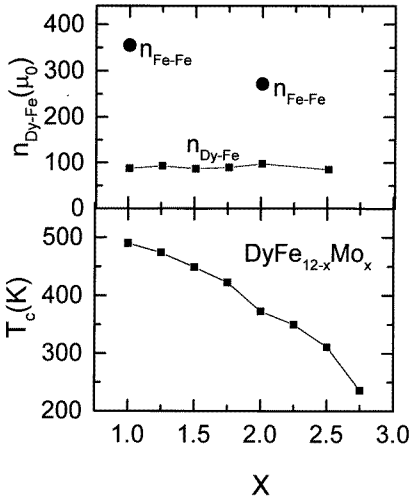

Figure 3. Mo concentration variation of Curie temperature T_C and molecular-field coefficient n_{Dy-Fe} for $DyFe_{12-x}Mo_x$.

keeps constant while n_{Fe-Fe} decreases with increasing Mo concentration. The average value of n_{Dy-Fe} is 90 μ_0 for $DyFe_{12-x}Mo_x$ and considerably smaller than n_{Fe-Fe} of 355 μ_0 and 272 μ_0 for $YFe_{11}Mo_1$ and $YFe_{10}Mo_2$ [15]. It indicates that the Fe–Fe exchange interaction is predominant in $DyFe_{12-x}Mo_x$.

The saturation magnetization M_s at 4.2 K and room temperature is given in table 1 and plotted in figure 4. figure 4 indicates that M_s decreases linearly with Mo concentration. Like Curie temperatures, M_s reduces more quickly than that calculated from the 'dilution model'. In this work, M_s of $DyFe_{11.0}Mo_{1.0}$ is 10.8 μ_B fu^{-1} and much smaller than the 23.7 μ_B fu^{-1} of $YFe_{11.0}Mo_{1.0}$ at 4.2 K. This is because of the ferrimagnetic coupling between Dy and Fe. Extrapolating x to 0, we obtain $M_s = 15.18$ μ_B fu^{-1} at 4.2 K for the hypothetical $DyFe_{12}$

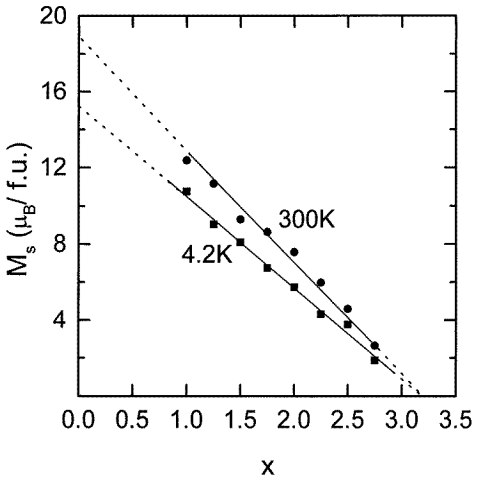

Figure 4. Mo concentration dependence of saturation magnetization M_s for $DyFe_{12-x}Mo_x$ at 4.2 K and room temperature.

compound, and extrapolating M_s to 0, we obtain critical concentration $x_{cr} = 3.2$ at which the ferromagnetic phase disappears in the $DyFe_{12-x}Mo_x$ compound. The value of $x_{cr} = 3.2$ is slightly smaller than $x_{cr} = 3.6$ which was calculated from the 'magnetic valence model' in $YFe_{12-x}Mo_x$ [15].

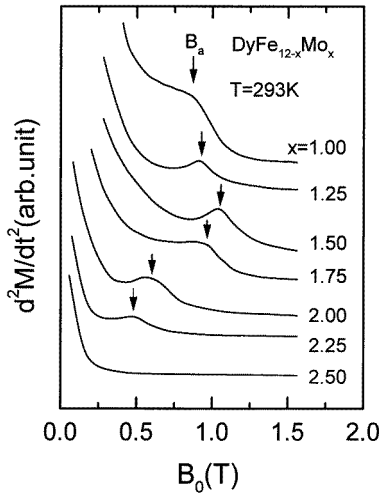

Figure 5. Typical SPD curves of $DyFe_{12-x}Mo_x$ at room temperature.

Figure 5 shows several typical room-temperature singular-point detection (SPD) curves on which the cusp indicates the magnetocrystalline anisotropy field B_a. The Mo concentration dependence of B_a is shown in figure 6. The x-ray diffraction patterns of aligned samples (see figure 1(b)) indicate that all the samples exhibit uniaxial anisotropy at room temperature though no peak is observed on the SPD curve for samples with $x = 2.50$ and 2.75. This results are good agreement with [11], [21] and [22] which considered

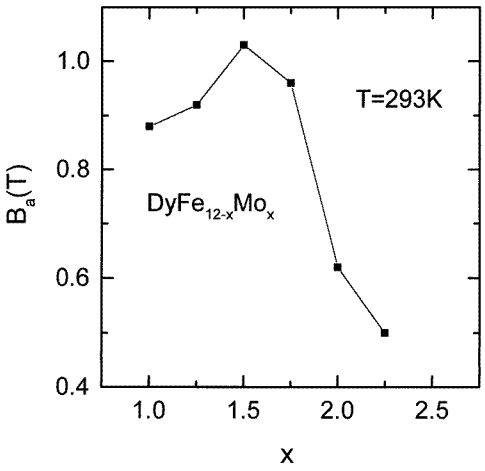

Figure 6. Mo concentration dependence of anisotropy field B_a for $DyFe_{12-x}Mo_x$ at room temperature.

the anisotropy as uniaxial for $DyFe_{10}Mo_2$, but somewhat different from [23] regarding $DyFe_{10}Mo_2$ as complex anisotropy at room temperature. In figure 6, B_a increases with Mo concentration at first and reaches a maximum at $x = 1.5$, then decreases rapidly with further increasing Mo concentration. This nonmonotonic variation in the Mo concentration dependence of the B_a for $DyFe_{12-x}Mo_x$ is very different from the linear relationship for $YFe_{12-x}Mo_x$ [19]. Since the magnetocrystalline anisotropy of the Fe sublattice decreases with increasing Mo concentration monotonically [19], so the maximum in the anisotropy of $DyFe_{12-x}Mo_x$ may be attributed to the variation of crystal-field interactions caused by the Dy sublattice. In our present work, B_a is 0.62 tesla for $x = 2$ at room temperature and near to the result of 0.42 tesla measured by Kou *et al* using the SPD technique [12] but remarkably smaller than that of 1.4 tesla which was obtained from the magnetization curves measured on the aligned samples by Tucker *et al* [22]. Moreover, at low temperatures a transition from uniaxial anisotropy to canted structure in samples with low Mo concentration ($x < 2$) and magnetohistory effects in samples with high Mo concentration ($x \geqslant 2$) were observed. Two typical examples of such change in samples were shown in figure 7 and figure 8. Figure 7 gives the angle φ dependence of the parallel component of magnetization, $M_\parallel$, for $DyFe_{10.75}Mo_{1.25}$ at several temperatures. It can be seen from figure 7 that the magnetically aligned sample $DyFe_{10.75}Mo_{1.25}$ still keeps a uniaxial anisotropy when the temperature decreases from 293 to 225 K since the $M_\parallel$ keeps a maximum at $\varphi = 0$ and a minimum at $\varphi = 90^\circ$. But when the temperature is below 175 K, the values of $M_\parallel$ at $\varphi = 90^\circ$ is no longer the minimum and the minima occur around $\varphi = \pm 60^\circ$ at temperatures of 125, 100 and 77 K. These changes imply that the easy magnetization direction of the aligned sample deviates from c-axis below 175 K. It indicates that the magnetic anisotropy changes from uniaxial to canted with decreasing temperature. The same magnetic phase transition from uniaxial to canted with decreasing temperature for $DyFe_{10}Mo_2$ has been observed in [12] and discussed in [13]. Figure 8 shows a temperature dependence of magnetization of $DyFe_{9.5}Mo_{2.5}$ alloy on cooling in a field of 0.1 tesla (FC) and zero field (ZFC). It follows from this result that a magnetohistory effect occurs in $DyFe_{9.5}Mo_{2.5}$ which has high Mo concentration. Further studies on the magnetocrystalline anisotropy and the magnetohistory effects for the $DyFe_{12-x}Mo_x$ series are in progress.

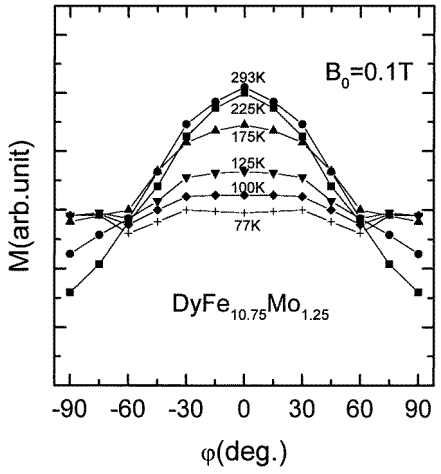

Figure 7. Parallel component of magnetization of magnetically aligned $DyFe_{10.75}Mo_{1.25}$ samples versus rotation angle with respect to the applied field ($B_0 = 0.1$ T).

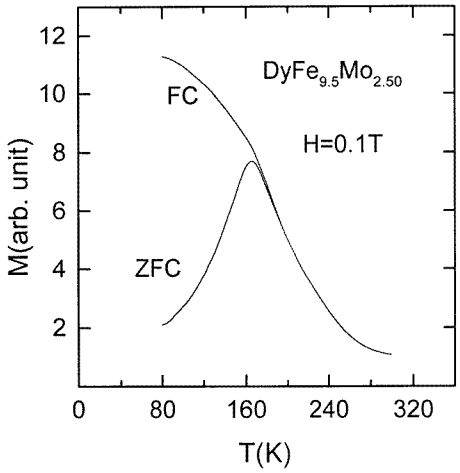

Figure 8. Temperature dependence of the magnetization of $DyFe_{9.5}Mo_{2.5}$ on zero-field cooling and field cooling.

In conclusion, crystallographic and magnetic properties of the $DyFe_{12-x}Mo_x$ series have been investigated in detail. All samples are single phase with the $ThMn_{12}$ type structure. With increasing Mo concentration, the lattice constants a and c increase linearly but with a different slope which is 0.0038 nm/Mo along the a-axis and 0.0026 nm/Mo along the c-axis. With increasing Mo concentration Curie temperature decreases monotonically and the saturation magnetization decreases linearly with 4.81 μ_B fu^{-1} per Mo atom. All the samples exhibit uniaxial anisotropy at room-temperature. The room-temperature anisotropy field varies in a non-linear way with increasing Mo concentration and a maximum value of 1.03 tesla appears at $x = 1.50$. At low temperature, $DyFe_{12-x}Mo_x$ compounds have a complex magnetic behaviour. A transition from uniaxial anisotropy to canted structure at low temperatures for samples with low Mo concentration ($x < 2$) and magnetohistory effects in samples with high Mo concentration ($x \geqslant 2$) was observed.

References

[1] Li Hong-Shou and Coey J M D 1991 *Handbook of Magnetic Materials* vol 6 (Elsevier)
[2] Buschow K H J and de Mooij D B 1989 *The Concerted European Action on Magnets (CEAM)* (London: Elsevier) p 63
[3] Hu B P, Wang K Y, Wang Y Z and Wang Z X 1995 *Phys. Rev.* B **51** 2905
[4] Verhoef R, de Boer F R, Zhang Z D and Buschow K H J 1988 *J. Magn. Magn. Mater.* **75** 319
[5] Christides C, Li H S, Kostikas A and Niarchos D 1991 *Physica* B **175** 329
[6] Christides C, Kostikas A, Zouganelis G and Psyharis V 1993 *Phys. Rev.* B **47** 1220
[7] Wang Y Z, Hu B P, Liu G C, Hu J H, Son L, Wang K Y and Lai W Y 1994 *J. Appl. Phys.* **76** 6383
[8] Wang Y Z, Hu B P, Rao X L, Liu G C, Son L, Yin L and Lai W Y 1994 *J. Appl. Phys.* **75** 6226
[9] Koestler C, Shultz L and Thomas G 1990 *J. Appl. Phys.* **67** 2532
[10] Anagnostou M, Christides C and Niamrchos D 1991 *Solid State Commun.* **78** 681
[11] Christides C, Kostikas A, Kou X C, Grössinger R and Niarchos D 1993 *J. Phys.: Condens. Matter* **5** 8611
[12] Kou X C, Grössinger R and Wiessinger 1995 *Phys. Rev.* B **51** 8254
[13] Guslienko K Yu, Sinnecker E H C P and Grössinger R 1997 *Phys. Rev.* B **55** 380
[14] Asti G and Rinaldi 1972 *Phys. Rev. Lett.* **28** 1584
[15] Sun Hong, Akayama M, Tatami K and Fujii H 1993 *Physica* B **183** 33
[16] Wang Y Z, Hadjipanayis G C, Tang Z X, Yelon W B, Papaefthymiou V, Moukarika A and Sellmyer D J 1993 *J. Magn. Magn. Mater.* **119** 41
[17] Sun Hong, Morri Y, Fujii H, Akayama M and Funahashi S 1993 *Phys. Rev.* B **48** 13 333
[18] Anagnostou M, Devlin E, Psycharis V, Kostikas A and Niarchos D 1994 *J. Magn. Magn. Mater.* **131** 157
[19] Wang Yi-Zhong, Hu Bo-Ping, Song Lin, Wang Kai-Ying and Liu Gui-Chuan 1994 *J. Phys.: Condens. Matter* **6** 7085
[20] Beloritzky E, Frémy M A, Gavigan J P, Givord D and Li H-S 1987 *J. Appl. Phys.* **61** 3971
[21] Kou X C, Christides C, Grössinger R, Kirchmayr H R and Kostikas A 1992 *J. Magn. Magn. Mater.* **104–107** 1341
[22] Tucker R, Xu Xie and Shaheen S A 1994 *J. Appl. Phys.* **75** 6229
[23] Yang Ying-Chang 1995 *Proc. 3rd Int. Symp. on Physics of Magnetic Materials, ISPMM'95 (Seoul, 1995)*